Improvement of Leaf Chlorophyll Content Estimation Using Spectral Indices From Nonpolarized Reflectance Factor in the Laboratory and Field

Yuefeng Li, Zhongqiu Sun, Shan Lu, and Kenji Omasa

***Abstract*—Optical properties of light reflected from leaves can be described by both intensity and polarization, however, most studies focused on the intensity in the estimation of plant leaf biochemical parameters. In this study, multiangular photometric and polarimetric measurements of leaves from three different plant species are first performed in laboratory to estimate leaf chlorophyll content (LCC) using spectral indices at different viewing zenith angles. Based on the Stokes parameters, the spectral indices in terms of the *I* parameter reflectance factors measured in laboratory ($\mathrm{IpRF_{lab}}$ if polarizer extinction is considered) can be used to estimate LCC, which has a similar accuracy as bidirectional reflectance factor (BRF); and the nonpolarized spectral proportion [the reduction of bidirectional polarized reflectance factor (BPRF) from IpRF (IpRF-BPRF)] improves the ability of the spectral indices, including single wavelength, simple ratio, simple difference and normalized difference indices, along with some other indices to estimate LCC using multiangular measurements. Subsequently, the field photometric and polarimetric measurements of leaves further confirm that the nonpolarized proportion improves the estimation of LCC for some spectral indices. These results not only provide evidence that the $\mathrm{IpRF_{lab}}$ and $\mathrm{IpRF_{field}}$ taken from polarimetric measurements can be considered as the proxy of photometric measurements (BRF and HDRF) in both laboratory and field but also open the possibility to improve the accuracy of LCC estimation using a nonpolarized spectral reflectance factor from multiangular polarimetric measurements. These findings indicate that polarized remote sensing may play a significant role in vegetation studies.**

***Index Terms*—Leaf chlorophyll content (LCC), multiangular measurements, polarimetric property, remote sensing, spectral indices.**

Manuscript received May 12, 2020; revised June 20, 2020; accepted June 21, 2020. Date of publication June 25, 2020; date of current version July 6, 2020. This work was supported in part by the National Natural Science Foundation of China under Grant 41971290, Grant 41771362, and Grant 41671347; in part by the Jilin Provincial Science and Technology Development Project under Grant 20180201012GX and Grant 20180101313JC; and in part by the Fundamental Research Funds for the Central Universities under Grant 130014925. *(Corresponding authors: Zhongqiu Sun; Shan Lu.)*

Yuefeng Li, Zhongqiu Sun, and Shan Lu are with the Key Laboratory of Geographical Processes and Ecological Security in Changbai Mountains, Ministry of Education, School of Geographical Science, Northeast Normal University, Changchun 130024, China (e-mail: liyf043@nenu.edu.cn; sunzq465@nenu.edu.cn; lus123@nenu.edu.cn).

Kenji Omasa is with the Graduate School of Agricultural and Life Sciences, The University of Tokyo, Tokyo 113-8657, Japan, and also with the Faculty of Agriculture, Takasaki University of Health and Welfare, Takasaki 370-0033, Japan (e-mail: aomasa@mail.ecc.u-tokyo.ac.jp).

This article has supplementary downloadable material available at http://ieeexplore.ieee.org, provided by the authors.

Digital Object Identifier 10.1109/JSTARS.2020.3004976

I. Introduction

LEAF pigment contents are typically used as indicators of plant physiological status and stresses and are therefore indicative of plant productivity. The determination of leaf pigment contents, such as chlorophyll, is an important performance metric in both plant physiology and plant ecology [1]–[3]. Optical measurements, which are rapid and noninvasive, have been widely used to estimate leaf chlorophyll content (LCC) at various spatial scales [4]–[17] because chlorophyll content changes the spectral reflectance of leaves [18]–[20]. Based on the relationship between LCC and reflectance [21], most studies have focused on reflectance as measured by intensity, using spectral indices when estimating LCC [22], [23]. However, except for the intensity, polarization is necessary for describing the reflected light from leaf [24]–[26].

Total reflectance from the leaf is characterized by two components: diffuse and specular, which can both be obtained using polarimetric measurements [27]–[30]. The specular component can be calculated by the combination of a polarized reflectance factor and the Fresnel equation. The diffuse component is then the difference between total reflectance and specular reflectance. The specular portion, arising from the leaf surface, dominates the polarized characterization of leaves. The diffuse portion, created through multiple scattering within a leaf, has a weak impact on the polarization of the leaf and is primarily related to nonpolarized reflectance [27], [28], [31], [32]. Therefore, information about the polarized component of reflected light is potentially related to leaf or vegetation surface structure properties [27], [52], [80], whereas the nonpolarized component may be useful for describing the inner components of the leaf, such as pigmentation [29], [33].

Reported studies have focused on the relationship between vegetation properties and polarization at different scales, such as in ground measurements of vegetation, the radiation transfer process [34]–[39], vegetation amount [40], and phenological condition [41]. Polarized signals from airborne and spaceborne measurements have also been used to characterize the polarization properties of vegetation [42]–[48]. The above-mentioned studies are primarily focused on the polarized proportion of reflectance from leaf surfaces, which has direct or indirect relationships with vegetation properties [34], [35], [41].

When measuring polarization, angular information is needed, which is then used to determine the dominant direction of

TABLE I
CHARACTERISTICS OF LEAF SAMPLES

Samples	Leaf shape	Surface properties
Pa	Oval	Relatively flat and smooth leaf surface, a glabrous surface with veins
Sm	Large, long oval.	Thick leathery, a smooth and glabrous surface
Ju	Oval or long oval.	Many veins, very sparse and fine hairs

reflectance at the leaf surface [49]–[52]. The leaf surface properties affect the accuracy of LCC estimates when measurements of the angular reflectance of leaves are used [53], [54]. To improve the ability of spectral indices to estimate LCC in different viewing directions across a wide variety of species, the difference between two wavelengths is usually used to reduce leaf surface reflectance [12], [55], [56]. Other indices, e.g., single wavelength (SW), simple ratio (SR), and normalized difference (ND) indices, cannot eliminate such impacts of surface reflectance, which lead to a decrease in accuracy of LCC estimates due to multiangular reflectance factor [54]. Although several studies indicated that the polarized reflectance portion of a leaf was derived primarily from the leaf surface [27], [28], [32], researchers did not investigate the relationship between the polarimetric measurements and photometric measurements of leaves in estimates of LCC basing on Stokes parameters, which can also separate the nonpolarized reflectance factor from the total reflectance factor. Thus, a detailed investigation of the relationships between LCC and the angular polarimetric spectral measurements of leaves is necessary for the spectroscopy community.

In this article, the Stokes parameters were used to describe the polarization properties of leaves. First, the *I* parameter reflectance factor measured in laboratory ($\mathrm{IpRF_{lab}}$) was used to compare with bidirectional reflectance factor (BRF) to indicate that if the BRF can be replaced by $\mathrm{IpRF_{lab}}$ when they are used to relate to LCC. We also examined if the nonpolarized spectral reflectance factor can improve the estimation of LCC when using spectral indices at different viewing directions in the laboratory condition. Then, the polarimetric measurements of leaves under different incident zenith angles were used to further confirm the effectivity of the nonpolarized reflectance factor for improving the estimation of LCC in the field condition.

II. SAMPLES AND METHODS

A. Leaf Samples

From April to October in 2018 and 2019, 175 samples were taken from three species of plants: *Pachira aquatica* (Pa, $n = 65$), *Schefflera microphylla Merr*. (Sm, $n = 55$), and *Juglans* (Ju, $n = 55$) in laboratory measurements. An additional 122 samples (Pa, $n = 44$; Sm, $n = 40$; and Ju, $n = 38$) were measured in the field. Fig. 1(a)–(i) illustrates nine samples with different LCCs. We used 130 calibration samples from laboratory, whereas 45 samples from the laboratory (15 samples from each species) and all of the field samples ($n = 122$) were used for validation. Sampled leaves were characterized as shown in Table I. The leaf surface characteristics of these three plant species are different from each other, which affect the reflectance factor distribution of leaves.

TABLE II
NOTATIONS USED FOR THE DEFINITION OF PHOTOMETRIC AND POLARIMETRIC QUANTITIES

Symbols	Description
L	Reflected radiance (W m^{-2} sr^{-1})
I	Total reflected radiance (W m^{-2} sr^{-1})
Q	Magnitude of the polarization ellipse semimajor axis
U	Orientation of the polarization ellipse semimajor axis
θ	Zenith angle (°)
φ	Azimuth angle (°)
λ	Wavelength (nm)
ρ	Hemispherical spectral reflectance of a Spectralon (dimensionless)
Subscripts	
s	Source
v	Viewing
0°, 45°, 90° and 135 °	Polarized radiance in the four polarizer directions
p	Polarized radiance
lab	Laboratory measurements
field	Field measurements
sample	Leaf sample
reference	Reference panel (Spectralon)
n-p	Non-polarized portion
terms	
BRF	Bidirectional reflectance factor
HDRF	Hemispherical directional reflectance factor
BPRF	Bidirectional polarized reflectance factor
IpRF	*I* parameter reflectance factor

B. Measurements

In laboratory measurements, the SZA was 40°, and the photometric and polarimetric properties of Sm and Ju leaves from 12 VZAs were measured in the principal plane (60°, 50°, 30°, 20°, 10°, 0°, −10°, −20°, −30°, −40°, −50°, and −60°, angles with "–" correspond to forward scattering directions). For the Pa leaves, the angular spectral reflectance factor was measured from ten VZAs (the measurements at 50° and 30° were not performed in the backward scattering direction), as shown in Fig. 1(o). Both photometric and polarimetric measurements were performed using the Northeast Normal University Laboratory Goniospectrometer System (NENULGS) [57] [see Fig. 1(n)]. Notations used for the definition of photometric and polarimetric quantities are shown in Table II.

The bidirectional reflectance factor ($\mathrm{BRF_{lab}}$) was used to characterize photometric properties of leaf samples in laboratory measurements. $\mathrm{BRF_{lab}}$ is defined as the ratio of reflected radiance ($dL_{\mathrm{lab,sample}}$) from the leaf to the reflected radiance ($dL_{\mathrm{lab,reference}}$) from an ideal diffuse reference surface (with the same area as the leaf sample) in the same viewing directions under single-direction illumination. This factor is calculated as follows [58]:

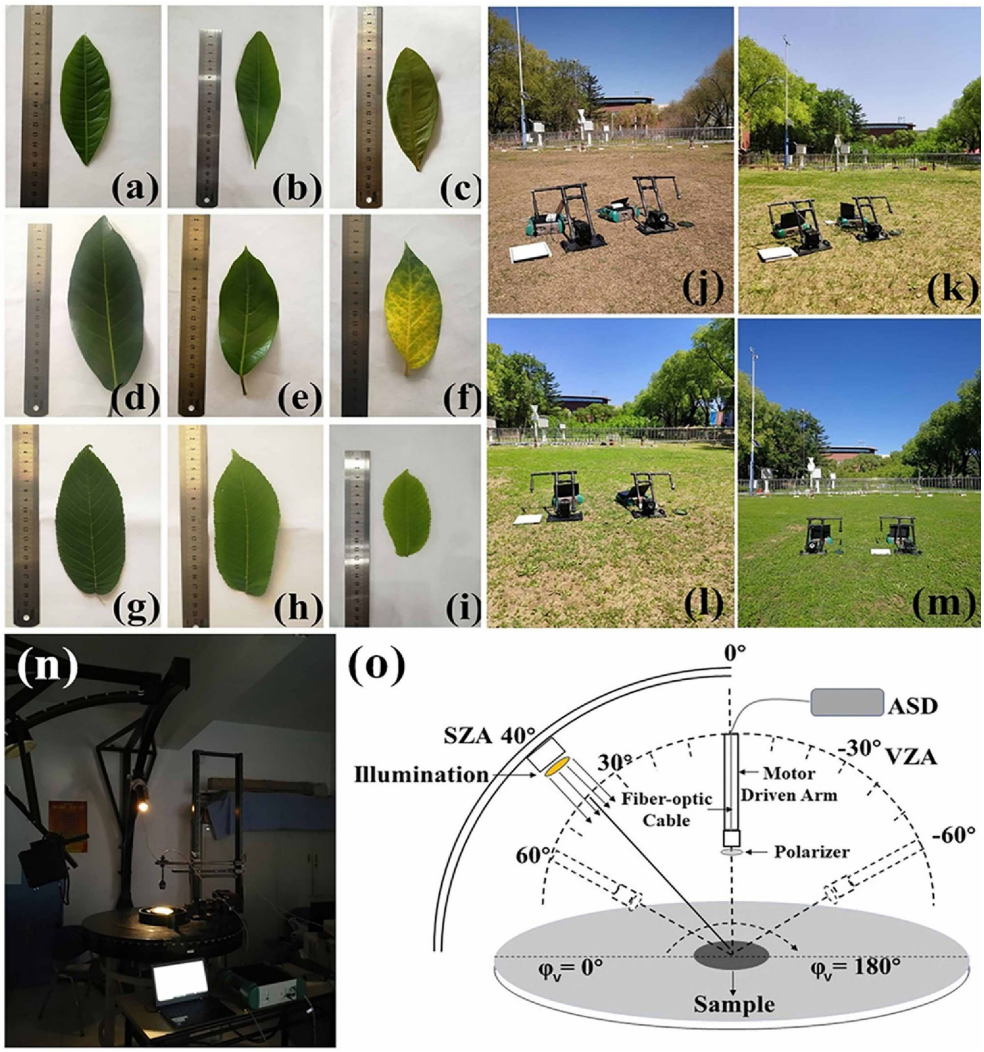

Fig. 1. Photographs of leaves with different chlorophyll content include Pa (a) 35.12, (b) 29.93, (c) 20.31 μg/cm^2; Sm (d) 73.42, (e) 38.80, (f) 7.26 μg/cm^2; and Ju (g) 49.72, (h) 32.07, and (i) 15.46 μg/cm^2, where Pa, Sm, and Ju are plant species. Field photographs (j)–(m) show multiangular measurements under different incident conditions (52°, 42°, 34°, and 23°) in the field, where one Analytical Spectral Devices (ASD) spectroradiometer was used to measure the reflected radiance from a Spectralon panel, and the other was used to measure photometric and polarimetric signals from leaves with the same measurement geometry. Image (n) illustrates laboratory measurements, whereas (o) shows a diagram of the system taking measurements in the principal plane in laboratory, where $\varphi v = 180°$ corresponds to the forward scattering direction. SZA and VZA correspond to the source zenith angle and viewing zenith angle, respectively.

$$\mathrm{BRF}_{\mathrm{lab}}(\lambda,\theta_s,\theta_v,\varphi_s,\varphi_v) = \frac{dL_{\mathrm{lab,sample}}(\lambda,\theta_s,\theta_v;\varphi_s,\varphi_v)}{dL_{\mathrm{lab,reference}}(\lambda,\theta_s,\theta_v;\varphi_s,\varphi_v)}\rho_\lambda. \quad (1)$$

The value of ρ_λ is about 0.99 provided by the manufacturer. Photometric measurements should be described by the biconical reflectance factor (BCRF) [58]. $\mathrm{BRF}_{\mathrm{lab}}$ of the leaves was considered similar to the BCRF, which were assumed in previous laboratory studies [59]–[60] [61].

There are three main components of the NENULGS: a goniometer, which varies the viewing angles of a sample's hemisphere, an ASD spectroradiometer (FieldSpec 3, Colorado, USA), and artificial illumination (Osram, halogen lamp 250 W, Germany), which provides collimated light by using a parabolic mirror and a convex mirror. The spectral reflectance factor has an average relative uncertainty of 1%, and linear polarization has an average relative uncertainty of less than 5% [57]. Detailed descriptions of NENULGS were included in a previous study [57]. The sampling process for a single leaf including photometric and polarimetric measurements took approximately 20 min. We assumed that variations in leaf properties did not affect measured results.

In field measurements, two goniometers coupled with two ASD spectroradiometers were used, as shown in Fig. 1(j)–(m), the SZA ranged from 23° to 52°. Both ASD spectroradiometers were calibrated before photometric and polarimetric measurements. One system measured the reflected radiance from the Spectralon panel as reference, whereas the other system measured the photometric and polarimetric reflected radiance from leaves in the principal plane. Both measurement systems used the same VZA. The hemispherical directional reflectance factor

($\mathrm{HDRF_{field}}$) was used to characterize the photometric properties of leaves in the field measurements. $\mathrm{HDRF_{field}}$ is similar to $\mathrm{BRF_{lab}}$, but it also includes irradiance from the hemisphere (2π) space [58], such that

$$\mathrm{HDRF_{field}}(\lambda,\theta_s,\theta_v,\varphi_s,\varphi_v) = \frac{dL_{\mathrm{field,sample}}(\lambda,2\pi,\theta_s,\theta_v;\varphi_s,\varphi_v)}{dL_{\mathrm{field,reference}}(\lambda,2\pi,\theta_s,\theta_v;\varphi_s,\varphi_v)}\rho_\lambda. \quad (2)$$

To avoid water loss under sunny conditions, leaf measurements were performed at only one, three, or five VZAs (from 0° to 60° in the forward scattering direction in the principal plane at 10° interval), which took no more than 4 min.

The main difference between the polarimetric and photometric measurements is that a polarizer is in front of the fiber of spectrometer for collecting polarized reflected radiance from leaves surfaces. Four Stokes parameters (*I*, *Q*, *U,* and *V*) are typically used to describe the polarimetric properties of the target surfaces. *V* is negligible after being reflected from the natural surface [25]

$$I = (L_{0^\circ} + L_{45^\circ} + L_{90^\circ} + L_{135^\circ})/2 \quad (3)$$

$$Q = L_{0^\circ} - L_{90^\circ} \quad (4)$$

$$U = L_{45^\circ} - L_{135^\circ} \quad (5)$$

$$L_{\mathrm{p}} = \sqrt{Q^2 + U^2}. \quad (6)$$

The reference plane is the meridional plane of the instrument. The polarizer was rotated with an accuracy of 1° from 0° to 360°. L_{p} is the polarized radiance, which can be used to define the bidirectional polarized reflectance factor (BPRF). BPRF is the ratio of the polarized reflected radiance ($dL_{\mathrm{p,sample}}$) of the leaf surface to the reflected radiance ($dL_{\mathrm{reference}}$) from the Spectralon panel (with the same area as the leaf sample) in the same viewing directions under single-direction illumination [39], [45], [46], [62]

$$\mathrm{BPRF}(\lambda,\theta_s,\theta_v,\phi_s,\phi_v) = \frac{dL_{\mathrm{p}}(\lambda,\theta_s,\theta_v;\phi_s,\phi_v)}{dL(\lambda,\theta_s,\theta_v;\phi_s,\phi_v)}\rho_\lambda. \quad (7)$$

In this article, the *I* parameter reflectance factor (IpRF) characterizes the sum of the polarized reflected radiance from four polarizer directions, as shown in (3). The definition of IpRF is similar to that of the $\mathrm{BRF_{lab}}$ in the laboratory and $\mathrm{HDRF_{field}}$ in the field, which are shown in (1) and (2), respectively. In the numerator of IpRF, dL_{sample} is replaced by dI_{sample}, as follows:

$$\mathrm{IpRF}(\lambda,\theta_s,\theta_v,\varphi_s,\varphi_v) = \frac{dI_{\mathrm{sample}}(\lambda,\theta_s,\theta_v;\varphi_s,\varphi_v)}{dL_{\mathrm{reference}}(\lambda,\theta_s,\theta_v;\varphi_s,\varphi_v)}\rho_\lambda. \quad (8)$$

Theoretically, $\mathrm{BRF_{lab}}$ or $\mathrm{HDRF_{field}}$ is equal to the IpRF in laboratory and field, but these reflectance factors are derived from different measurement processes. When measuring IpRF, there is a polarizer in front of the spectrometer fiber-optic cable, and polarizer extinction decreases polarized radiance in the four different polarizer directions. The polarizer extinction ($\mathrm{ext_{polarizer}}$) is calculated by comparing the difference between radiance of the Spectralon panel measured with polarizer and without polarizer [62]

$$\mathrm{ext_{polarizer}} = 1 - L_{\mathrm{spectralon,polarizer}}/L_{\mathrm{spectralon}}. \quad (9)$$

$L_{\mathrm{spectralon}}$ is the reflected radiance of the Spectralon without a polarizer. Then, the average of polarized reflected radiance of Spectralon at four polarizer directions (0°, 45°, 90°, or 135°) was used to calculate $L_{\mathrm{spectralon,polarizer}}$, $L_{\mathrm{spectralon,\ polarizer}} = (L_{\mathrm{spectralon},0^\circ} + L_{\mathrm{spectralon},\ 45^\circ} + L_{\mathrm{spectralon},90^\circ} + L_{\mathrm{spectralon},135^\circ})/4$. The detailed description can be referred to a previous reference [62].

Ignoring the polarizer extinction, *I* parameter is calculated as (3). Adding the polarizer extinction, *I* parameter changes to the following:

$$I_{\mathrm{sample,true}} = \left(\frac{L_{0^\circ}}{1-\mathrm{ext_{polarizer}}} + \frac{L_{45^\circ}}{1-\mathrm{ext_{polarizer}}} + \frac{L_{90^\circ}}{1-\mathrm{ext_{polarizer}}} + \frac{L_{135^\circ}}{1-\mathrm{ext_{polarizer}}}\right)/2. \quad (10)$$

Then, IpRF shown in (8) can be defined as (8) and (12) for laboratory and field conditions

$$\mathrm{IpRF_{lab}}(\lambda,\theta_s,\theta_v,\varphi_s,\varphi_v) = \frac{dI_{\mathrm{lab,sample,true}}(\lambda,\theta_s,\theta_v;\varphi_s,\varphi_v)}{dL_{\mathrm{reference}}(\lambda,\theta_s,\theta_v;\varphi_s,\varphi_v)}\rho_\lambda \quad (11)$$

$$\mathrm{IpRF_{field}}(\lambda,\theta_s,\theta_v,\varphi_s,\varphi_v) = \frac{dI_{\mathrm{field,sample,true}}(\lambda,2\pi,\theta_s,\theta_v;\varphi_s,\varphi_v)}{dL_{\mathrm{field,reference}}(\lambda,2\pi,\theta_s,\theta_v;\varphi_s,\varphi_v)}\rho_\lambda. \quad (12)$$

Comparing (8) (without considering polarizer extinction) with (11) and (12) (considering polarizer extinction), if the polarizer extinction is excluded, the $\mathrm{IpRF_{lab}}$ and $\mathrm{IpRF_{field}}$ will be smaller than the $\mathrm{BRF_{lab}}$ ($\mathrm{HDRF_{field}}$) of a target surface at all wavelengths.

If the $\mathrm{IpRF_{lab}}$ ($\mathrm{IpRF_{field}}$) is able to estimate LCC estimation as well as $\mathrm{BRF_{lab}}$ ($\mathrm{HDRF_{field}}$), both intensity and polarized properties of a leaf from polarimetric measurements can be obtained. In addition, the nonpolarized portion of the reflectance factor ($\mathrm{BRF_{lab,n\text{-}p}}$ and $\mathrm{HDRF_{field,n\text{-}p}}$) can be obtained directly from the difference between $\mathrm{IpRF_{lab}}$ ($\mathrm{IpRF_{field}}$) and the $\mathrm{BPRF_{lab}}$ ($\mathrm{BPRF_{field}}$) in both the laboratory and the field as follows:

$$\mathrm{BRF_{lab,n-p}} = \mathrm{BRF_{lab}} - \mathrm{BPRF_{lab}} = \mathrm{IpRF_{lab}} - \mathrm{BPRF_{lab}} \quad (13)$$

$$\mathrm{HDRF_{field,n-p}} = \mathrm{HDRF_{field}} - \mathrm{BPRF_{field}} = \mathrm{IpRF_{field}} - \mathrm{BPRF_{field}}. \quad (14)$$

There were 52 leaf samples used to compare $\mathrm{HDRF_{field}}$ and $\mathrm{IpRF_{field}}$, and both photometric and polarimetric measurements were performed in the field. Only polarimetric measurements were taken for the remaining 70 samples. Hereafter, $\mathrm{IpRF_{lab}}$ and $\mathrm{IpRF_{field}}$ of leaves mean that both laboratory and field measurements result with the consideration of polarizer extinction.

To keep the measured area smaller than the leaf area, the field of view was fixed at 6°, and the distance from the detector to the

TABLE III
STATISTICAL RESULTS OF ALL LEAF SAMPLE CHLOROPHYLL CONTENTS IN THE LABORATORY, 130 CALIBRATION SAMPLES WERE RELATED TO SPECTRAL INDICES

	Sample number	Max Chl (μg/cm²)	Min Chl (μg/cm²)	Means (μg/cm²)	Standard Deviation	Coefficient of Variation
Laboratory measurements						
Calibration						
Sm	40	73.42	1.11	42.18	18.49	0.44
Ju	40	50.29	13.88	28.58	11.05	0.39
Pa	50	40.45	6.10	22.14	10.68	0.48
Total	130	73.42	1.11	30.29	16.02	0.53
Validation						
Sm	15	71.83	7.26	34.70	19.05	0.55
Ju	15	48.81	15.69	31.53	9.78	0.31
Pa	15	45.85	7.57	26.34	11.58	0.44
Total	45	71.83	7.26	30.86	14.47	0.47
Field measurements						
Sm	40	78.39	7.01	53.27	14.45	0.27
Pa	44	49.03	3.03	31.43	12.43	0.40
Ju	38	63.18	0.18	29.32	16.13	0.55
Total	122	78.39	0.18	37.93	14.33	0.38

There were additional 45 validation samples, leading to a total sample size of 175. A total of 122 samples were taken from field measurements. Pa, Sm, and Ju are plant species.

leaf sample was 0.2 m for both the laboratory and field measurements. These conditions changed the footprint in the detector from a circular area with a diameter of 2.1 cm to an elliptical area with a length of 4.2 cm when the VZA changed from 0° to 60°. To eliminate background effects on measurements, the leaf, which had a main vein in the center of the measured area in the principal plane, was placed on an objective stage covered by a black-tape board. The reflectance factor of the black-tape board is less than 0.05 and independent of wavelength. During measurements, we did not press leaf surfaces down to keep them flat; we placed only the two ends of the leaves on the objective stage. Spectral wavelengths from 400 to 1000 nm were used in this study.

C. LCC Measurements

After measuring the photometric and polarimetric properties of the leaf, three pieces were cut from the measurement area using a 6-mm diameter hole punch. The leaf samples were ground in a clear mortar, and the leaf pigment mixture was placed in a 25 ml volumetric flask with 95% ethanol. The solution and chlorophyll mix were placed in a plastic tube, and then the tube was placed in a centrifuge with a rotation speed of 3200 r/min for 10 min. A Lambda 900 spectrophotometer (Perkin-Elmer, Waltham, MA, USA) was used to measure the supernatant absorption to calculate the LCC (μg/cm^2) using the method provided by the previous study [63]. The LCC statistical results for both the laboratory and filed are shown in Table III. Because the photometric and polarimetric properties of leaves in the field were measured at random directions (with a 10° interval) in the principal plane, the samples measured at different VZA are with different chlorophyll content, as shown in Table S1 in supplementary.

D. Spectral Indices

In this study, 21 spectral indices were used to estimate LCC based on photometric and polarimetric spectral measurements (see Table IV). The spectral indices can be generalized into six types: SW, derivative (D), SR, SD, ND, and other indices [12]. The 21 existing spectral indices will be used to calculated LCC across all viewing directions using $\mathrm{BRF_{lab}}$ ($\mathrm{HDRF_{field}}$), $\mathrm{IpRF_{lab}}$

TABLE IV
SPECTRAL INDICES USED IN THIS STUDY INCLUDE SW, DERIVATIVE (D), SR, SIMPLE DIFFERENCE INDICES (SD), AND ND, ALONG WITH SIX OTHER SPECTRAL INDICES

Type	Spectral indices	Sources
SW	$1/R_{700}$	[64]
D	D_{730}	[65]
SR	R_{750}/R_{550}	[66]
	R_{750}/R_{700}	[66]
	R_{860}/R_{550}	[67]
	R_{800}/R_{680}	[68]
	R_{800}/R_{635}	[68]
	R_{750}/R_{710}	[11]
	R_{950}/R_{680}	[69]
	R_{750}/R_{705}	[12]
SD	$1/R_{550}$-$1/R_{750}$	[9]
	$1/R_{700}$-$1/R_{750}$	[9]
ND	$(R_{750}$-$R_{705})/(R_{750}$+$R_{705})$	[8]
	$(R_{800}$-$R_{650})/(R_{800}$+$R_{650})$	[70]
	$(R_{800}$-$R_{635})/(R_{800}$+$R_{635})$	[68]
Others	$(R_{750}$-$R_{705})/(R_{750}$+R_{705}-$2R_{445})$	[12]
	$R_{860}/(R_{550}$*$R_{708})$	[67]
	$(R_{734}$-$R_{747})/(R_{715}$+$R_{726})$	[10]
	$R_{705}/(R_{717}$+$R_{491})$	[71]
	$(R_{850}$-$R_{710})/(R_{850}$-$R_{680})$	[56]
	$(R_{750}$-$R_{445})/(R_{705}$-$R_{445})$	[12]

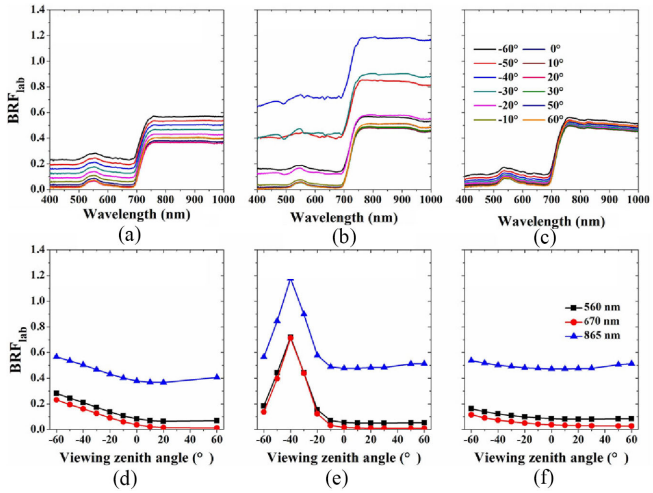

Fig. 2. Spectral BRF_{lab} of leaves from three plant species (a) Pa, (b) Sm, and (c) Ju, at 12 different VZAs, and the BRF_{lab} distribution for (d) Pa, (e) Sm, and (f) Ju, at selected wavelengths (560, 670, and 865 nm) at different VZAs are shown. The incident angle was 40°, and the angles were measured in the principal plane, "–" corresponds to the forward scattering directions. Pa, Sm, and Ju are plant species.

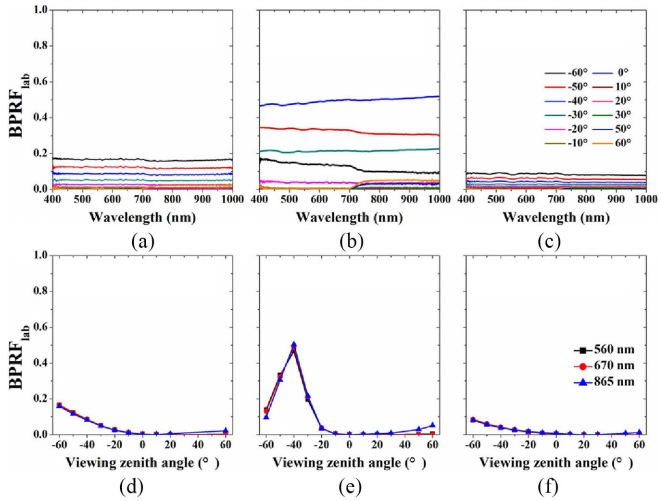

Fig. 3. Spectral $BPRF_{lab}$ of leaves from three plant species in the laboratory, (a) Pa, (b) Sm, and (c) Ju, at different VZAs. The distribution of the $BPRF_{lab}$ of leaves, (d) Pa, (e) Sm, and (f) Ju, at three selected wavelengths (560, 670, and 865 nm) at different VZAs. The incident angle was 40°, "–" corresponds to the forward scattering directions. Pa, Sm, and Ju are plant species.

($IpRF_{field}$) and $BRF_{lab,n\text{-}p}$ ($HDRF_{field,n\text{-}p}$). The determination coefficient (R^2) was used during calibration to explain the relationship between spectral indices and LCC. Root-mean-square error (RMSE) was used to evaluate prediction accuracy by comparing measured and estimated LCC.

III. Results

A. Angular Spectral Reflection and Polarization of Leaf Samples

Fig. 2(a)–(c) shows spectral BRF_{lab} of three leaf samples at different VZAs in the principal plane. The location of the maximum spectral reflectance factor of these leaf samples was in the forward scattering direction, whereas the minimum spectral reflectance factor was found in the nadir or backward scattering directions. To examine the distribution pattern of reflectance factor of leaves from different plant species, BRF_{lab} at selected wavelengths (560, 670, and 865 nm) is displayed in Fig. 2(d)–(f). The Sm leaf has a strong specular peak when the SZA equals the VZA (–40°). The maximum BRF_{lab} of the Pa leaf spreads across the specular peak, and the Ju leaf has a weak angular reflectance pattern. Based on these results in Fig. 2, it is found that the Sm leaf had the strongest anisotropic characteristic, followed by the Pa leaf, and then the Ju leaf. These three species of leaves with differing angular reflectance properties were used to investigate the relationship between the spectral indices and LCC at different VZAs.

The $BPRF_{lab}$ and $BPRF_{field}$ of leaves and vegetation covers have been confirmed to be approximately spectrally neutral [30], [32], [35], [72], [73]. Fig. 3 shows the spectral $BPRF_{lab}$ of the three leaf samples at different VZAs in the principal plane in the laboratory. Clearly, the $BPRF_{lab}$ of leaves from the three different plant species [see Fig. 3(a)–(c)] is not completely independent of wavelength, because of the leaf surface

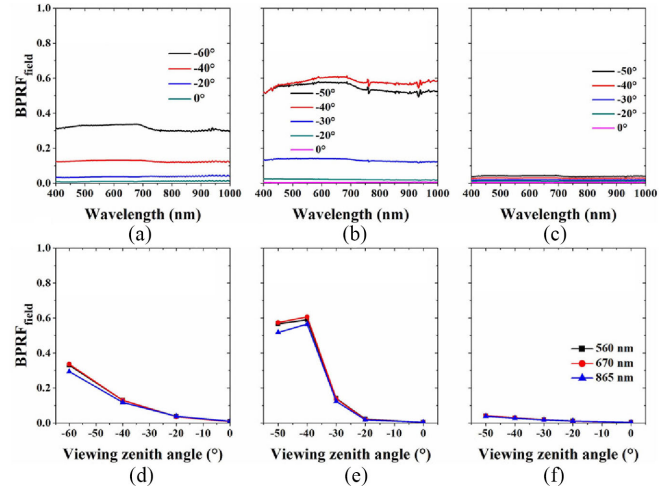

Fig. 4. Spectral $BPRF_{field}$ of leaves from three plant species in the field, (a) Pa, (b) Sm, and (c) Ju, at different VZAs. The distribution of $BPRF_{field}$ at selected wavelength of leaves (560, 670, and 865 nm) for the three leaves, (d) Pa, (e) Sm, and (f) Ju, at different VZAs in the principal plane. Pa, Sm, and Ju are plant species.

refractive index as a function of the wavelength, which leads to the variation of BPRF at different wavelengths [52]. The weak dependence of wavelength was also measured for the $BPRF_{field}$ for leaves in the field [see Fig. 4(a)–(c)]. This similar wavelength-dependent $BPRF_{field}$ for vegetation has also been found by Ground-based Multiangle SpectroPolarimetric Imager [74]. Moreover, the $BPRF_{lab}$ and $BPRF_{field}$ at different wavelengths vary with the VZA in Figs. 3(d)–(f) and 4(d)–(f). This is because Sm has a smooth surface and Ju has a rough surface, the smoother the surface, the more the specular reflection. The polarization properties of leaves will be used to calculate the nonpolarized reflectance factor from the total reflectance factor.

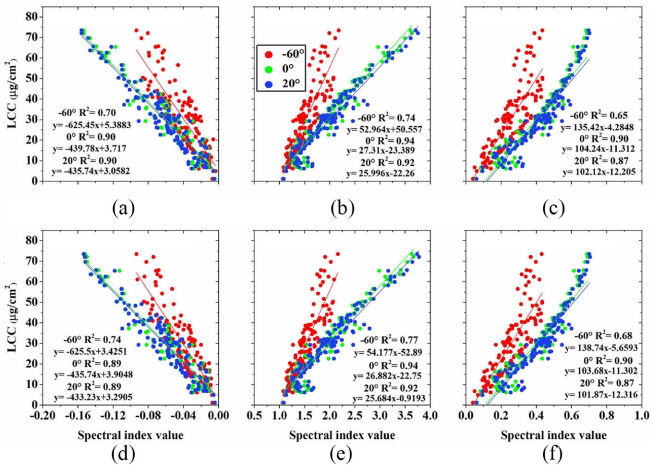

Fig. 5. Relationships between LCC and selected spectral indices in terms of (a)–(c) BRF_{lab} and (d)–(f) $IpRF_{lab}$ at different VZAs, $n = 130$. The three selected VZAs represent the forward scattering (–60°), nadir (0°), and backward scattering (20°) directions; combining with similar R^2, the similar slope values of the formula further confirmed the similarity between BRF_{lab} and $IpRF_{lab}$ in different viewing directions.

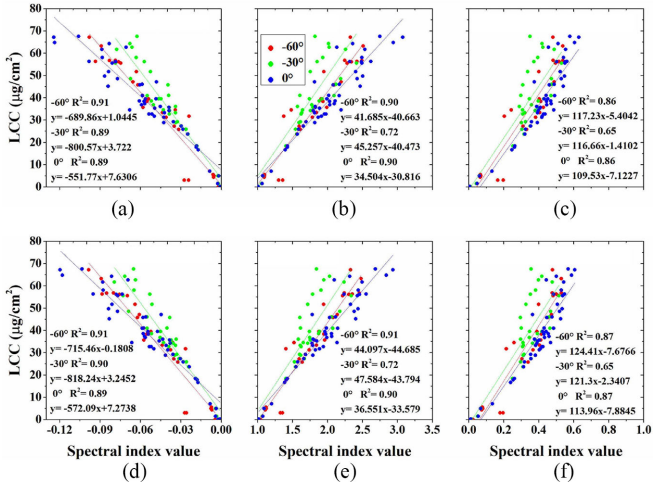

Fig. 6. Relationship between LCC and selected spectral indices in terms of (a)–(c) $HDRF_{field}$ and (d)–(f) $IpRF_{field}$ at three different VZAs, $n = 49$ for 0°, $n = 32$ for –30°, and $n = 25$ for –60°. Except for R^2, the slopes of $HDRF_{field}$ and $IpRF_{field}$ are similar to each other for the field measurements.

B. Relationship of Spectral Indices With LCC in Terms of BRF and IpRF

The R^2 values and slope values of the relationships between the LCC and three selected indices in terms of BRF_{lab} and $IpRF_{lab}$ at different VZAs are shown in Fig. 5. The similar R^2 values and slope values from different spectral indices at different VZAs indicate that the relationship is similar when using $IpRF_{lab}$ and BRF_{lab} to relate to LCC. The relationships (R^2_{BRFlab}) between spectral indices in terms of BRF_{lab} and LCC for all calibration samples, and the relationships ($R^2_{IpRFlab}$) between spectral indices and LCC in terms of $IpRF_{lab}$ for all calibration samples are summarized in Table S2 in supplementary. The relationships of the spectral indices with LCC are similar for both BRF_{lab} and $IpRF_{lab}$ in each viewing direction and in all ten measurement directions, these results further illustrate that the BRF_{lab} can be replaced by $IpRF_{lab}$. The other interesting finding is that the relationships between most of the spectral indices and LCC depend on the VZAs, especially in the forward scattering directions (see Fig. 5 and Table S2 in supplementary).

Comparisons of $R^2_{HDRFfield}$ and $R^2_{IpRFfield}$ for $HDRF_{field}$ and $IpRF_{field}$ of leaves in field measurements were also made (see Fig. 6). Similar R^2 values and slope values are found in Fig. 6, further confirming that the $HDRF_{field}$ can be replaced by $IpRF_{field}$ when polarizer extinction is included. Nine spectral indices with significance ($P < 0.001$) at all seven viewing directions and total direction were selected in Table S3 in supplementary, similar relationship with LCC was found for both $HDRF_{field}$ and $IpRF_{field}$ of leaves. In this study, $HDRF_{field}$ and $IpRF_{field}$ are just used to demonstrate that they have similar relationships to LCC in field measurements. The similarity of relationships is because the reflectance factors derived from photometric and polarimetric measurements are similar when considering the polarizer extinction (see Fig. S1 in supplementary), the average relative difference between the BRF_{lab} ($HDRF_{field}$) and $IpRF_{lab}$ ($IpRF_{field}$) of all leaf samples across the wavelength range from 400 to 1000 nm was within 5%.

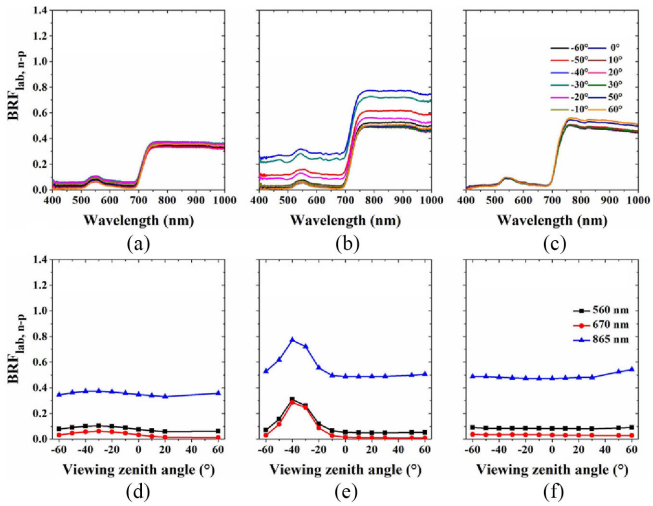

Fig. 7. Spectral $BRF_{lab,n-p}$ of three plant species leaves, (a) Pa, (b) Sm, and (c) Ju, at different VZAs, and the distribution of $BRF_{lab,n-p}$ of leaves, (d) Pa, (e) Sm, and (f) Ju, at selected wavelengths (560, 670, and 865 nm) at different VZAs. The *Y*-axis value range is the same as in Fig. 2.

C. Relationship Between Spectral Indices and LCC With Respect to the Nonpolarized Reflectance Factor

Following the replacement of BRF_{lab} (or $HDRF_{field}$) with $IpRF_{lab}$ (or $IpRF_{field}$) for both laboratory and field leaf samples, the nonpolarized spectral reflectance factor, $BRF_{lab,n-p}$ ($HDRF_{field,n-p}$), of the leaf samples in one direction is calculated by the difference between $IpRF_{lab}$ ($IpRF_{field}$) and $BPRF_{lab}$ ($BPRF_{field}$). The spectral $BRF_{lab,n-p}$ values (Fig. 7(a)–(c); range of 0–0.8) are lower than the BRF_{lab} of the leaves (Fig. 2(a)–(c); range of 0–1.2) in each viewing direction, whereas $BRF_{lab,n-p}$ at selected wavelengths [see Fig. 7(d)–(f)] is less sensitive to viewing direction than the BRF_{lab} [see Fig. 2(d)–(f)].

TABLE V
R^2_{IpRFlab} AND $R^2_{\mathrm{BRFlab,n\text{-}p}}$ FOR 130 CALIBRATION SAMPLES IN THE LABORATORY

Spectral indices	Data type	-60°	-50°	-40°	-30°	-20°	-10°	0°	10°	20°	60°	Average	Total
D_{730}	R^2_{IpRFlab}	**0.82**	**0.83**	**0.82**	**0.83**	**0.83**	**0.83**	**0.84**	**0.85**	**0.85**	**0.86**	**0.84**	**0.82**
	$R^2_{\mathrm{BRFlab,\,n\text{-}p}}$	**0.85**	**0.85**	**0.77**	**0.74**	**0.81**	**0.83**	**0.85**	**0.85**	**0.85**	**0.83**	**0.82**	**0.82**
R_{750}/R_{710}	R^2_{IpRFlab}	**0.77**	**0.23**	**0.09**	**0.27**	**0.85**	**0.94**	**0.94**	**0.93**	**0.92**	**0.90**	**0.68**	**0.52**
	$R^2_{\mathrm{BRFlab,\,n\text{-}p}}$	**0.93**	**0.75**	**0.35**	**0.53**	**0.89**	**0.94**	**0.94**	**0.93**	**0.92**	**0.90**	**0.81**	**0.75**
R_{750}/R_{705}	R^2_{IpRFlab}	**0.67**	**0.14**	0.05*	**0.17**	**0.80**	**0.94**	**0.94**	**0.93**	**0.92**	**0.91**	**0.64**	**0.47**
	$R^2_{\mathrm{BRFlab,\,n\text{-}p}}$	**0.93**	**0.64**	**0.24**	**0.41**	**0.86**	**0.94**	**0.94**	**0.94**	**0.92**	**0.91**	**0.77**	**0.70**
$(R_{750}\text{-}R_{705})/(R_{750}+R_{705})$	R^2_{IpRFlab}	**0.65**	**0.16**	0.04*	**0.21**	**0.78**	**0.90**	**0.90**	**0.89**	**0.88**	**0.86**	**0.62**	**0.44**
	$R^2_{\mathrm{BRFlab,\,n\text{-}p}}$	**0.88**	**0.65**	**0.29**	**0.47**	**0.83**	**0.90**	**0.90**	**0.89**	**0.88**	**0.86**	**0.76**	**0.70**
$(R_{750}\text{-}R_{705})/(R_{750}+R_{705}\text{-}2R_{445})$	R^2_{IpRFlab}	**0.90**	**0.75**	**0.55**	**0.79**	**0.88**	**0.87**	**0.86**	**0.86**	**0.85**	**0.85**	**0.82**	**0.81**
	$R^2_{\mathrm{BRFlab,\,n\text{-}p}}$	**0.87**	**0.85**	**0.79**	**0.84**	**0.88**	**0.87**	**0.87**	**0.87**	**0.86**	**0.86**	**0.86**	**0.85**
$(R_{734}\text{-}R_{747})/(R_{715}+R_{726})$	R^2_{IpRFlab}	**0.74**	**0.31**	0.08*	**0.19**	**0.74**	**0.87**	**0.89**	**0.89**	**0.89**	**0.91**	**0.64**	**0.54**
	$R^2_{\mathrm{BRFlab,\,n\text{-}p}}$	**0.92**	**0.82**	**0.53**	**0.59**	**0.84**	**0.89**	**0.89**	**0.88**	**0.88**	**0.90**	**0.81**	**0.79**
$R_{705}/(R_{717}+R_{491})$	R^2_{IpRFlab}	**0.82**	**0.65**	**0.51**	**0.62**	**0.80**	**0.83**	**0.83**	**0.82**	**0.81**	**0.81**	**0.75**	**0.70**
	$R^2_{\mathrm{BRFlab,\,n\text{-}p}}$	**0.82**	**0.76**	**0.68**	**0.72**	**0.81**	**0.83**	**0.82**	**0.82**	**0.81**	**0.81**	**0.79**	**0.78**
$(R_{850}\text{-}R_{710})/(R_{850}\text{-}R_{680})$	R^2_{IpRFlab}	**0.88**	**0.87**	**0.88**	**0.88**	**0.88**	**0.88**	**0.88**	**0.87**	**0.87**	**0.85**	**0.87**	**0.87**
	$R^2_{\mathrm{BRFlab,\,n\text{-}p}}$	**0.89**	**0.89**	**0.88**	**0.88**	**0.88**	**0.88**	**0.88**	**0.87**	**0.87**	**0.85**	**0.88**	**0.88**
$(R_{750}\text{-}R_{445})/(R_{705}\text{-}R_{445})$	R^2_{IpRFlab}	**0.76**	**0.86**	**0.53**	**0.86**	**0.90**	**0.92**	**0.92**	**0.92**	**0.92**	**0.91**	**0.85**	**0.76**
	$R^2_{\mathrm{BRFlab,\,n\text{-}p}}$	**0.93**	**0.92**	**0.85**	**0.90**	**0.91**	**0.92**	**0.92**	**0.92**	**0.92**	**0.91**	**0.91**	**0.90**
Average	R^2_{IpRFlab}	**0.77**	**0.53**	**0.37**	**0.53**	**0.82**	**0.88**	**0.88**	**0.88**	**0.87**	**0.86**	**0.74**	**0.65**
	$R^2_{\mathrm{BRFlab,\,n\text{-}p}}$	**0.88**	**0.78**	**0.59**	**0.67**	**0.85**	**0.88**	**0.88**	**0.88**	**0.87**	**0.86**	**0.81**	**0.79**

"–" represents the forward scattering directions in the principal plane. Significance is indicated as, $P = 0.001$–0.05 $(*)$ and $P < 0.001$(bold text). The average R^2 (in column) of all indices at each VZA and the average R^2 (in row) of each index over all VZA are also used to illustrate nonpolarized reflectance factor improve the relationship between several indices and LCC.

The relationships between the nine spectral indices (using $\mathrm{IpRF_{lab}}$ and $\mathrm{BRF_{lab,n\text{-}p}}$) and LCC at different VZAs and across all viewing directions are shown in Table V. The $R^2_{\mathrm{BRFlab,n\text{-}p}}$ values of most spectral indices in the forward scattering directions are much larger than the R^2_{IpRF} values. Improved relationships between the spectral indices in terms of $\mathrm{BRF_{lab,n\text{-}p}}$ and LCC in these forward scattering directions also lead to relatively high $R^2_{\mathrm{BRFlab,n\text{-}p}}$ when the samples from all measurement directions are combined, as shown in the comparison between Fig. 8(a)–(c) and Fig. 8(d)–(f). The top three plots are obtained from spectral indices in terms of $\mathrm{IpRF_{lab}}$ and LCC, whereas the bottom three plots are obtained from spectral indices in terms of $\mathrm{BRF_{lab,n\text{-}p}}$ and LCC in different viewing directions. As the field results show in Table S4 in supplementary, improvement for most spectral indices was also found in forward scattering directions, leading to an increase of R^2 values and the change of slope value when all directions were combined (see Fig. S2 in supplementary) using $\mathrm{HDRF_{field,n\text{-}p}}$.

The relationships (Table V and Table S4 in supplementary) between the spectral indices and LCC in terms of total reflectance factors ($\mathrm{IpRF_{lab}}$ and $\mathrm{IpRF_{field}}$) and nonpolarized reflectance factors ($\mathrm{BRF_{lab,n\text{-}p}}$ and $\mathrm{HDRF_{field,n\text{-}p}}$) under both laboratory and field conditions indicate that relationship between most spectral indices and LCC is improved when the nonpolarized reflectance factor is used. This improvement occurs at different VAZs (mainly in the forward scattering directions) and over all directions in the principal plane.

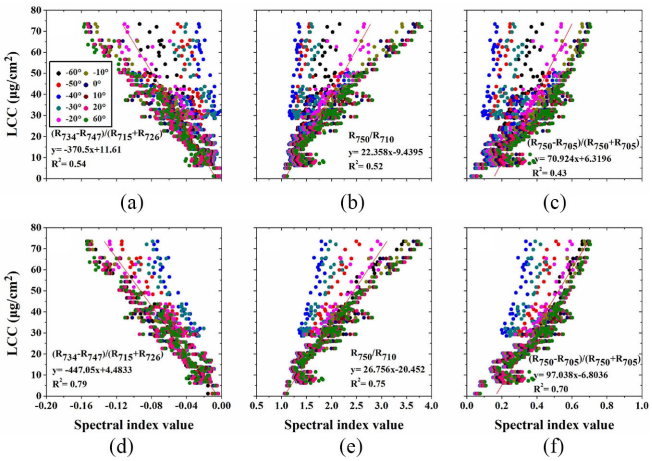

Fig. 8. Relationships of spectral indices with LCC in terms of (a)–(c) $\mathrm{IpRF_{lab}}$ and in terms of (d)–(f) $\mathrm{BRF_{lab,n\text{-}p}}$ for all measurement directions. Different colors indicate results at different VZAs ($n = 130$).

D. Improvement of LCC Estimation Using Nonpolarized Reflectance Factors

Comparing the RMSE obtained from the $\mathrm{IpRF_{lab}}$ in Fig. 9(a), estimation of LCC improved in the forward scattering directions for the three plant species when $\mathrm{BRF_{lab,n\text{-}p}}$ was used under laboratory condition [see Fig. 9(b)]. For each plant species, the RMSEs calculated using $\mathrm{IpRF_{lab}}$ and $\mathrm{BRF_{lab,n\text{-}p}}$ at each VZA

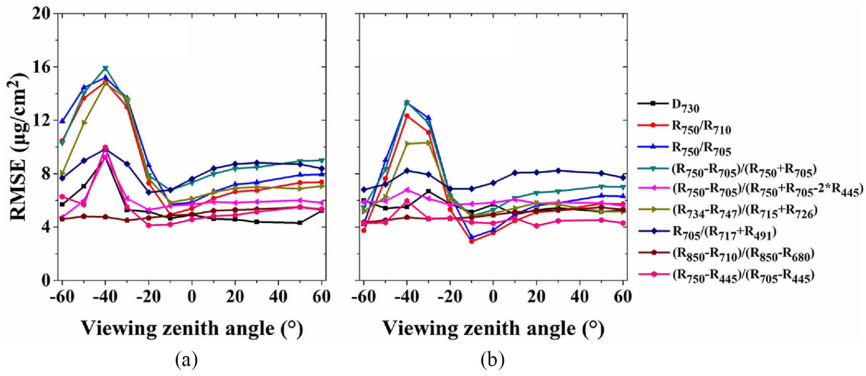

Fig. 9. RMSE of the estimated LCC ($n = 45$) from three plant species in each viewing direction, using the formula obtained from the combination of all calibration samples over all measurement directions. (a) $\mathrm{IpRF_{lab}}$ and (b) $\mathrm{BRF_{lab,n\text{-}p}}$ of validation samples at VZAs of 30° and 50° in the backward scattering direction were measured and used in the validation process.

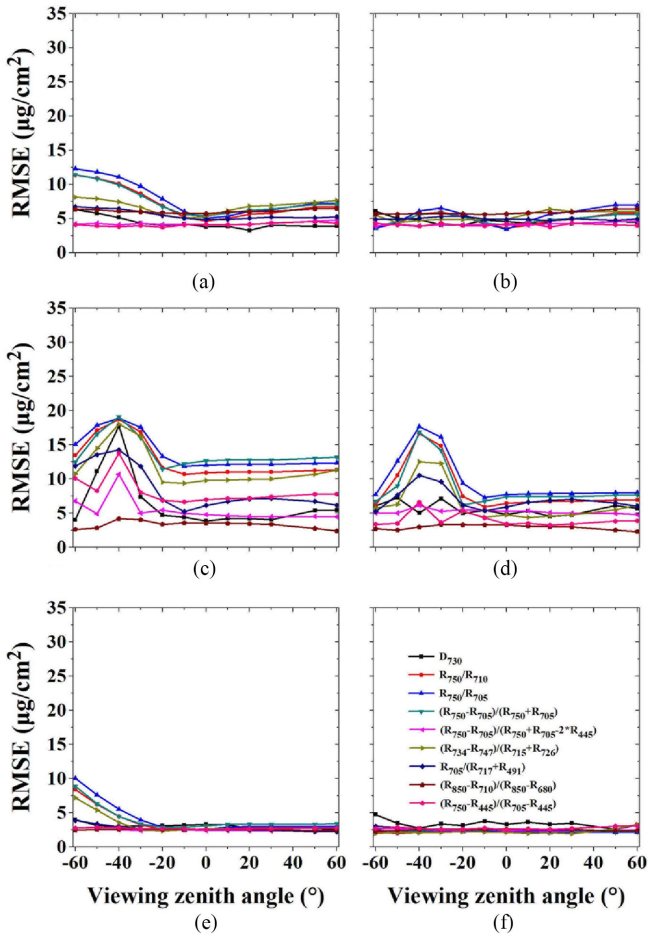

Fig. 10. RMSEs of estimated LCC in terms of (a), (c), and (e) $\mathrm{IpRF_{lab}}$ and (b), (d), and (f) $\mathrm{BRF_{lab,n\text{-}p}}$ for each plant species at different VZAs. RMSE values of some spectral indices using $\mathrm{BRF_{lab,n\text{-}p}}$ are smaller than values from $\mathrm{IpRF_{lab}}$. Pa, Sm, and Ju are plant species.

are shown in Fig. 10. The RMSE dependence on the VZA in Fig. 10 is very similar to the distributions of $\mathrm{IpRF_{lab}}$ [same to $\mathrm{BRF_{lab}}$ in Fig. 2(d)–(f)] and $\mathrm{BRF_{lab,n\text{-}p}}$ [see Fig. 7(d)–(f)] of leaves from each plant species. This result indicates that the estimated LCC results based on $\mathrm{BRF_{lab,n\text{-}p}}$ are not as sensitive to angular information as that based on $\mathrm{IpRF_{lab}}$, and then $\mathrm{BRF_{lab,n\text{-}p}}$ improves the accuracy of LCC estimation.

Moreover, the improvement of LCC estimation using nonpolarized reflectance factor was also validated to the field measurements. Comparing the RMSE obtained from the $\mathrm{IpRF_{field}}$ [see Fig. 11(a)] and the $\mathrm{HDRF_{field,n\text{-}p}}$ [see Fig. 11(b)], it is found that the estimates of LCC improved in the forward scattering directions for the three plant species. The better estimation of LCC was also found for using $\mathrm{HDRF_{field,n\text{-}p}}$ than using $\mathrm{IpRF_{field}}$ for each plant species at each VZA, as shown in Fig. 12. In summary, using $\mathrm{BRF_{lab,n\text{-}p}}$ and $\mathrm{HDRF_{field,n\text{-}p}}$ improve the ability of LCC estimation for all spectral indices that cannot remove leaf surface reflectance, such as, SW, SR, SD, and ND indices. For the index, $(\mathrm{R_{750}}–\mathrm{R_{445}})/(\mathrm{R_{705}}–\mathrm{R_{445}})$, which can remove leaf surface reflectance, using nonpolarized reflectance factors also improve its ability of LCC estimation accuracy [see Figs. 9(b) and 11(b)]. This special case is discussed in the following section.

IV. Discussion

A. Analysis of Angular Spectral Reflectance Factor and Polarization of Leaf Samples

The magnitude and distribution of leaf angular reflectance are determined by leaf surface properties [49], [75]. Thus, there is a clear difference in the $\mathrm{BRF_{lab}}$ among the three species of leaves (see Fig. 2). In fact, specular reflectance dominates the total reflectance of leaves at different VZAs in the forward scattering direction, and it also controls the polarization properties of leaf surfaces [28], [35]. This phenomenon is confirmed by the fact that the $\mathrm{BPRF_{lab}}$ distribution of the three leaf species [see Fig. 3(d)–(f)] is very similar to the $\mathrm{BRF_{lab}}$ distribution of the three leaf species [see Fig. 2(d)–(f)].

However, the $\mathrm{BRF_{lab}}$ ($\mathrm{HDRF_{field}}$) and polarization properties were taken by different measurement process, the former was directly calculated by the reflected radiance, the later was obtained from polarized radiance at four different directions using a polarizer. If the $\mathrm{BRF_{lab}}$ ($\mathrm{HDRF_{field}}$) can be replaced by $\mathrm{IpRF_{lab}}$ ($\mathrm{IpRF_{field}}$) for leaves at different VZAs when performing polarimetric measurements, we can achieve the goal of this study:

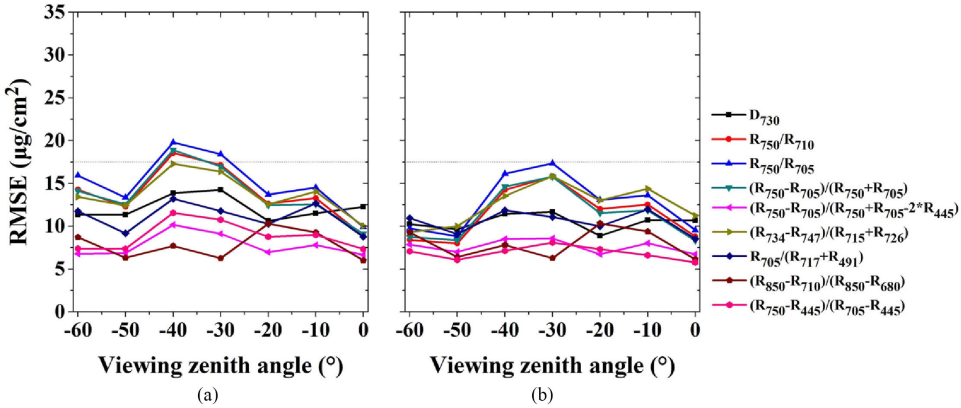

Fig. 11. RMSE of the estimated LCC from three plant species ($n = 122$) in each viewing direction basing on (a) $\mathrm{IpRF_{field}}$ and (b) $\mathrm{HDRF_{field,n\text{-}p}}$, using the same formulas as Fig. 9(a) and (b).

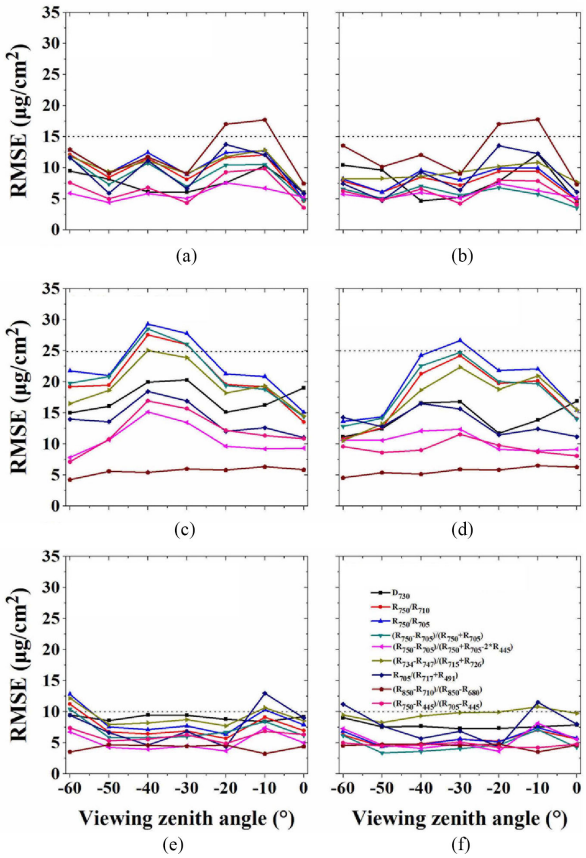

Fig. 12. RMSEs of estimated LCC based on (a), (c), and (e) $\mathrm{IpRF_{field}}$ and (b), (d), and (f) $\mathrm{HDRF_{field,n\text{-}p}}$ are shown for each plant species at different VZAs. RMSE values of some spectral indices calculated using the $\mathrm{HDRF_{field,n\text{-}p}}$ are smaller than the values based on $\mathrm{IpRF_{field}}$ ($n = 122$).

using $\mathrm{BRF_{lab,n\text{-}p}}$ and $\mathrm{HDRF_{field,n\text{-}p}}$ to estimate LCC based on only polarimetric measurements at different VZAs.

B. Replacement of BRF_{lab} ($HDRF_{field}$) With $IpRF_{lab}$ ($IpRF_{field}$) to Estimate LCC

The Stokes parameters are usually used to describe the polarization properties of reflected light from natural surfaces [42], [47], [72], [76], and IpRF, which is, in theory, the same as the reflectance factor obtained from photometric measurements. In previous study [62], researchers confirmed that the values of $\mathrm{IpRF_{lab}}$ were similar to the values of $\mathrm{BRF_{lab}}$ for several target surfaces when polarizer extinction was included. In this study, the $\mathrm{IpRF_{lab}}$ ($\mathrm{IpRF_{field}}$) of leaves with different LCCs is also similar to the $\mathrm{BRF_{lab}}$ ($\mathrm{HDRF_{field}}$) of leaves across all wavelengths (400–1000 nm). After confirming that the relationships of spectral indices to LCC using $\mathrm{IpRF_{lab}}$ ($\mathrm{IpRF_{field}}$) and $\mathrm{BRF_{lab}}$ ($\mathrm{HDRF_{field}}$) are also similar for individual direction and across all viewing directions (see Figs. 5 and 6), the RMSE values calculated by $\mathrm{BRF_{lab}}$ and $\mathrm{IpRF_{lab}}$ [see Fig. 9(a) and (b)] are similar at each VZA. Thus, reflectance factor, polarized and nonpolarized reflectance factors of a leaf in individual directions can be derived from polarimetric measurements when polarizer extinction is considered in both laboratory and field conditions.

C. Using Nonpolarized Reflectance Factor to Improve Estimates of LCC

There is a clear dependence on viewing angle for the relationship (see Fig. 5, Table V, and Table S4 in supplementary) between most spectral indices (in terms of $\mathrm{BRF_{lab}}$ and $\mathrm{HDRF_{field}}$) and either estimated or measured LCC. These indices are SW, SR, SD, and the normalized ND indices. These spectral indices cannot remove leaf surface reflectance (or specular reflectance), which decreases the sensitivity of the spectral indices to LCC. Thus, the relationships (R^2) and estimated results (RMSE) follow the angular reflectance factor distribution of leaves. The more anisotropic the leaf reflectance factor, the more the relationships weaken and estimates become less accurate.

Basing on the finding that $\mathrm{BRF_{lab,n\text{-}p}}$ improves the estimation of LCC in laboratory (see Figs. 9 and 10), the study extends to the field measurements (see Figs. 11 and 12), which further confirms that $\mathrm{HDRF_{field,n\text{-}p}}$ improves the estimation of LCC in field condition. This is due to the specular reflectance is partly polarized, the $\mathrm{BPRF_{lab}}$ and $\mathrm{BPRF_{field}}$ can partially correct the specular reflectance. The $\mathrm{BPRF_{lab}}$ and $\mathrm{BPRF_{field}}$ do not convey information about the internal properties of leaves [27], [28], [52], [80]. Using the nonpolarized reflectance factor, which

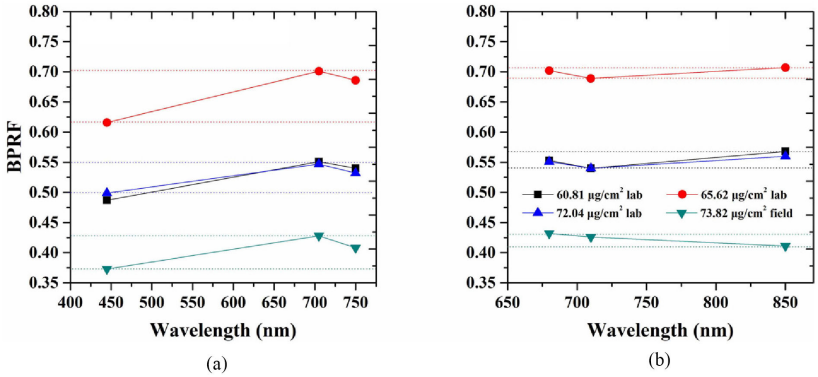

Fig. 13. Variation of BPRF values of Sm leaves with different LCC at different wavelengths for two spectral indices: (a) $(R_{750}–R_{445})/(R_{705}–R_{445})$ and (b) $(R_{850}–R_{710})/(R_{850}–R_{680})$. A large BPRF variation is found for $(R_{750}–R_{445})/(R_{705}–R_{445})$. The VZA is –40°. The differences between $BPRF_{lab}$ ($BPRF_{field}$) at 445, 705, and 750 nm are larger than that at 680, 710, and 850 nm.

emanates from within the leaf, improves the ability of spectral indices to estimate LCC, especially when viewing angles are dominated by specular reflectance.

D. Improvement of LCC Estimation Using the Spectral Index That Can Reduce Leaf Surface Reflectance

Assuming that specular reflectance does not depend on wavelength, researchers have used the spectral indices as ratios of the difference in reflectance to reduce the specular component (or leaf surface reflectance) and improve estimates of LCC based on spectral indices across a wide range of plant species [12], [55], [56], [77], [78]. Theoretically, if the specular reflectance from the leaf surface is independent of wavelength, the estimates of LCC resulting from spectral indices, such as $(R_{750}–R_{445})/(R_{705}–R_{445})$ and $(R_{850}–R_{710})/(R_{850}–R_{680})$, based on $IpRF_{lab}$ ($IpRF_{field}$), should be similar to that based on $BRF_{lab,n\text{-}p}$ ($HDRF_{field,n\text{-}p}$). However, for $(R_{750}–R_{445})/(R_{705}–R_{445})$, improved estimates of LCC were found using $BRF_{n\text{-}p}$ and $HDRF_{field,n\text{-}p}$ when compared with results using $IpRF_{lab}$ and $IpRF_{field}$ in the forward scattering directions (see Figs. 9 and 11). The improved result occurred for $(R_{750}–R_{445})/(R_{705}–R_{445})$ is due to the large differences between $BPRF_{lab}$ ($BPRF_{field}$) at 445, 705, and 750 nm for Sm leaves with high LCCs (see Fig. 13). The large differences between $BPRF_{lab}$ ($BPRF_{field}$) at 445, 705, and 750 nm decrease the relationship between $(R_{750}–R_{445})/(R_{705}–R_{445})$ (in terms of $IpRF_{lab}$ and $IpRF_{field}$) and LCC (see Fig. 14), and resulted in an increase of LCC estimation accuracy after separating the $BPRF_{lab}$ ($BPRF_{field}$) of leaves. In contrast, small differences between $BPRF_{lab}$ ($BPRF_{field}$) at 680, 710, and 850 nm have a weak influence on the relationship between $(R_{850}–R_{710})/(R_{850}–R_{680})$ and LCC, regardless of the $IpRF_{lab}$ ($IpRF_{field}$) or the $BRF_{lab,n\text{-}p}$ ($HDRF_{field,n\text{-}p}$) was used, the LCC estimation results are similar (see Fig. 15). These results indicate that the nonpolarized reflectance factors also improve the LCC estimation accuracy of spectral index, $(R_{750}–R_{445})/(R_{705}–R_{445})$, in which the difference between polarized reflectance factors of selected wavelengths is large, because using $BPRF_{lab}$ ($BPRF_{field}$) to describe specular reflectance is more accurate and practical than the assumption that specular reflectance is complete spectral neutral.

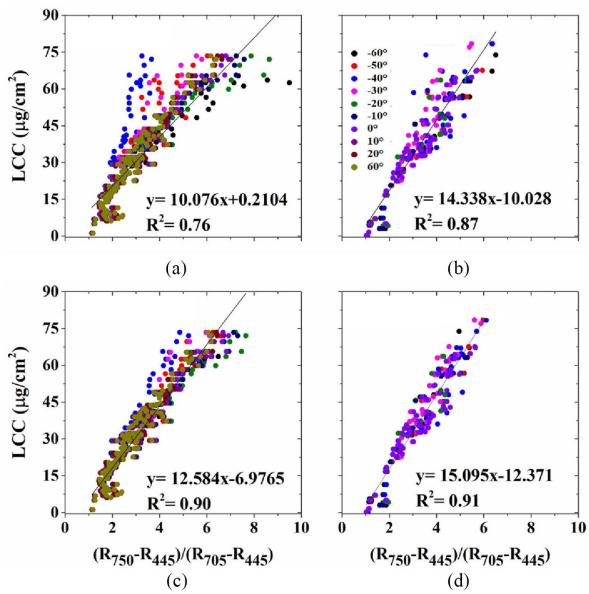

Fig. 14. Relationships between $(R_{750}–R_{445})/(R_{705}–R_{445})$ and LCC in terms of (a) $IpRF_{lab}$, (b) $IpRF_{filed}$, (c) $BRF_{lab,n\text{-}p}$, and (d) $HDRF_{field,n\text{-}p}$, $n = 130$ in laboratory measurements, $n = 122$ in field measurements. Because of the large differences between $BPRF_{lab}$ ($BPRF_{field}$) at 445, 705, and 750 nm at –40° VZA [Fig. 13(a)], $BRF_{lab,n\text{-}p}$ and $HDRF_{field,n\text{-}p}$ improve the relationships with LCC; see –40° with bright blue color in (c) and (d).

Several studies have indicated that the measured BPRF of leaves is not completely independent of wavelengths [29], [32], [35], [41], [62] because leaf surface properties, such as small wax particles and facets of wax particles, may change the polarization at some wavelengths. Thus, for spectral indices, which are considered as reducing leaf surface reflectance in theory, if the polarized reflectance factors of selected wavelengths with large difference, using nonpolarized reflectance factors also improves the LCC estimation accuracy. For spectral indices (SW, SR, SD, ND, and some others indices), which cannot reduce leaf surface reflectance, nonpolarized reflectance factors will certainly improve the LCC estimation accuracy based on multiangular polarimetric measurements. This is because the separation of polarized reflectance can reduce the specular reflectance from leaf surface.

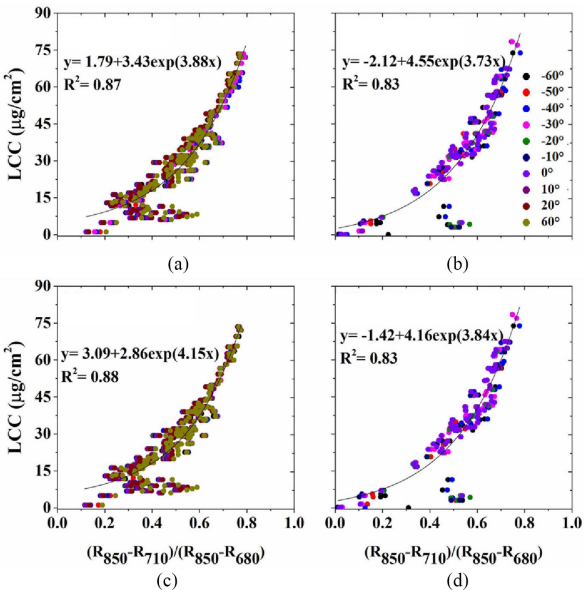

Fig. 15. Relationships between $(R_{850}–R_{710})/(R_{850}–R_{680})$ and LCC in terms of (a) $IpRF_{lab}$, (b) $IpRF_{filed}$, (c) $BRF_{lab,n-p}$, and (d) $HDRF_{field,n-p}$. The relationship is exponential, because only the reflection at 680 nm is dependent on LCC, and the dependence on LCC is exponential [52]. Small difference between $BPRF_{lab}$ ($BPRF_{field}$) at 680, 710, and 850 nm does not affect the relationship between $(R_{850}–R_{710})/(R_{850}–R_{680})$ and LCC when $BRF_{lab,n-p}$ and $HDRF_{field,n-p}$ are used.

E. Value of Polarimetric Measurement of Leaves on the LCC Estimation

Several existing studies used leaf clip and integrating sphere to estimate LCC, these methods could avoid the influence of specular reflection on LCC estimates [12], [55], [56], [77], [78]. However, considering the random leaf angles and varied sun incident zenith angles, even though the measurements were performed in the nadir direction, the angular reflection was, in fact, used to relate to LCC [22], [79]. Leaf specular reflection decreases the LCC estimates using the spectral indices that cannot remove the influence of specular reflection, such as SW, SR, SD, and the normalized ND indices. Using polarimetric measurements, researchers can obtain both intensity and polarization properties of leaves, and then calculate the nonpolarized reflectance factor, which avoids the limitation of the selection of spectral indices in the measured directions dominated by specular reflection. Thus, polarimetric properties of leaves allow researcher to estimate LCC using several effective methods under different conditions, then play a key role in the plant science, which needs accurate LCC results.

V. Conclusion

Polarimetric and photometric measurements of leaves with different chlorophyll contents from three plant species were taken, and these signals were used to estimate LCC using several spectral indices. The $IpRF_{lab}$ and $IpRF_{field}$, derived from polarimetric measurements, were proven to be similar to the BRF_{lab} in the laboratory and the $HDRF_{field}$ in the field in this study when the polarizer extinction is considered. For most spectral indices, the accuracy of estimates has a clear angular dependence that is based on multiangular measurements. Then, in both laboratory and field conditions, it is confirmed that BRF_{n-p} and $HDRF_{field,n-p}$ can weaken the angular dependence of some spectral indices on the accuracy of LCC estimation and improve the ability of those spectral indices to estimate LCC using multiangular measurements, especially in the forward scattering direction, which is dominated by specular reflectance.

Although polarimetric measurements require more time than photometric measurements, it is still valuable for vegetation remote sensing applications, because the reflectance factor as well as the polarized and nonpolarized reflectance factors in each viewing direction can be simultaneously obtained from polarimetric measurements by considering polarizer extinction. Combined with spectral information, we not only fully describe the optical properties of leaves, but also improve the ability of spectral indices to estimate LCC using BRF_{n-p} and $HDRF_{field,n-p}$. Because of the major differences in the surface structure of our selected leaf samples, we expect that more accurate estimates of LCC using nonpolarized reflectance factor can be found for other species when multiangular polarimetric measurements are performed. This study opens the possibility of detecting leaf biochemical properties using polarimetric measurements and indicates the importance of polarimetric signals to the spectroscopy community and vegetation remote sensing.

Acknowledgment

The authors would like to thank Prof. W. Yeqiao (University of Rhode Island) for several valuable comments on this study. Laboratory data have been uploaded to https://doi.org/10.6084/m9.figshare.11900322.v1 and Field data of this study are available; requests for data should be addressed to S. Lu and Z. Sun.

References

[1] H. Croft, J. M. Chen, X. Luo, P. Bartlett, B. Chen, and R. M. Staebler, "Leaf chlorophyll content as a proxy for leaf photosynthetic capacity," *Global Change Biol.*, vol. 23, no. 9, pp. 3513–3524, Sep. 2017.

[2] X. Luo, H. Croft, J. M. Chen, P. Bartlett, R. Staebler, and N. Froelich, "Incorporating leaf chlorophyll content into a two-leaf terrestrial biosphere model for estimating carbon and water fluxes at a forest site," *Agricultural Forest Meteorol.*, vol. 248, pp. 156–168, 2018.

[3] Y. Inoue *et al.*, "Simple and robust methods for remote sensing of canopy chlorophyll content: A comparative analysis of hyperspectral data for different types of vegetation," *Plant Cell Environ.*, vol. 39, no. 12, pp. 2609–2623, Dec. 2016.

[4] P. J. Curran, J. L. Dungan, and D. L. Peterson, "Estimating the foliar biochemical concentration of leaves with reflectance spectrometry: Testing the Kokaly and Clark methodologies," *Remote Sens. Environ.*, vol. 76, pp. 349–359, 2001.

[5] P. J. Curran, J. L. Dungan, and H. L. Gholz, "Exploring the relationship between reflectance red edge and chlorophyll content in slash pine," *Tree Physiol.*, vol. 7, pp. 33–48, 1990.

[6] I. Filella and J. Penuelas, "The red edge position and shape as indicators of plant chlorophyll content, biomass and hydric status," *Int. J. Remote Sens.*, vol. 15, no. 7, pp. 1459–1470, 1994.

[7] J. A. Gamon and J. S. Surfus, "Assessing leaf pigment content and activity with a reflectometer," *New Phytologist*, vol. 143, pp. 105–117, 1999.

[8] A. Gitelson and M. N. Merzlyak, "Spectral reflectance changes associated with autumn senescence of *Aesculus Hippocastanum L.* and *Acer platanoides L.* leaves. Spectral features and relation to chlorophyll estimation," *J. Plant Physiol.*, vol. 143, no. 3, pp. 286–292, 1994.

[9] A. A. Gitelson, Y. Gritz, and M. N. Merzlyak, "Relationships between leaf chlorophyll content and spectral reflectance and algorithms for non-destructive chlorophyll assessment in higher plant leaves," *J. Plant Physiol.*, vol. 160, no. 3, pp. 271–282, Mar. 2003.

[10] J. E. Vogelmann, B. N. Rock, and D. M. Moss, "Red edge spectral measurements from sugar maple leaves," *Int. J. Remote Sens.*, vol. 14, no. 8, pp. 1563–1575, 1993.

[11] P. Zarco-Tejada *et al.*, "Assessing vineyard condition with hyperspectral indices: Leaf and canopy reflectance simulation in a row-structured discontinuous canopy," *Remote Sens. Environ.*, vol. 99, no. 3, pp. 271–287, 2005.

[12] D. A. Sims and J. A. Gamon, "Relationships between leaf pigment content and spectral reflectance across a wide range of species, leaf structures and developmental stages," *Remote Sens. Environ.*, vol. 81, pp. 337–354, 2002.

[13] R. Casa, F. Castaldi, S. Pascucci, and S. Pignatti, "Chlorophyll estimation in field crops: An assessment of handheld leaf meters and spectral reflectance measurements," *J. Agricultural Sci.*, vol. 153, no. 5, pp. 876–890, 2014.

[14] C. E. Doughty *et al.*, "Can leaf spectroscopy predict leaf and forest traits along a Peruvian tropical forest elevation gradient?" *J. Geophys. Res., Biogeosci.*, vol. 122, no. 11, pp. 2952–2965, 2017.

[15] O. Mutanga and A. K. Skidmore, "Red edge shift and biochemical content in grass canopies," *ISPRS J. Photogramm. Remote Sens.*, vol. 62, no. 1, pp. 34–42, 2007.

[16] T. W. Gara, A. K. Skidmore, R. Darvishzadeh, and T. Wang, "Leaf to canopy upscaling approach affects the estimation of canopy traits," *GISci. Remote Sens.*, vol. 56, pp. 554–575, 2019.

[17] J. Penuelas, S. Munne-Bosch, J. Llusia, and I. Filella, "Leaf reflectance and photo- and antioxidant protection in field-grown summer stressed Phillyrea angustifolia. Optical signals of oxidative stress?" *New Phytologist*, vol. 162, pp. 115–124, 2004.

[18] P. J. Curran, "Multispectral remote sensing of vegetation amount," *Prog. Phys. Geography*, vol. 4, no. 3, pp. 315–341, 1980.

[19] C. J. Tucker, "Red and photographic infrared linear combinations for monitoring vegetation," *Remote Sens. Environ.*, vol. 8, no. 2, pp. 127–150, 1979.

[20] J. Penuelas, J. A. Gamon, K. L. Griffin, and C. B. Field, "Assessing community type, plant biomass, pigment composition and photosynthetic efficiency of aquatic vegetation from spectral reflectance," *Remote Sens. Environ.*, vol. 46, pp. 110–118, 1993.

[21] A. Gitelson and A. Solovchenko, "Generic algorithms for estimating foliar pigment content," *Geophys. Res. Lett.*, vol. 44, no. 18, pp. 9293–9298, 2017, doi: 10.1002/2017gl074799.

[22] F. M. Muharam, T. Delahunty, and S. J. Maas, "Evaluation of nitrogen treatment effects on the reflectance of cotton at different spatial scales," *Int. J. Remote Sens.*, vol. 39, no. 23, pp. 8482–8504, 2018.

[23] L. Hallik, T. Kazantsev, A. Kuusk, J. Galmés, M. Tomás, and Ü. Niinemets, "Generality of relationships between leaf pigment contents and spectral vegetation indices in Mallorca (Spain)," *Regional Environ. Change*, vol. 17, no. 7, pp. 2097–2109, 2017.

[24] J. S. Tyo, D. L. Goldstein, D. B. Chenault, and J. A. Shaw, "Review of passive imaging polarimetry for remote sensing applications," *Appl. Opt.*, vol. 45, no. 22, pp. 5453–5469, 2006.

[25] D. A. Talmage and P. J. Curran, "Remote sensing using partially polarized light," *Internal J. Remote Sens.*, vol. 7, no. 1, pp. 47–64, 1986.

[26] J. T. Woolley, "Reflectance and transmittance of light by leaves," *Plant Physiol.*, vol. 47, no. 5, pp. 656–662, 1971.

[27] V. C. Vanderbilt, L. Grant, and C. S. T. Daughtry, "Polarization of light scattered by vegetation," *Proc. IEEE*, vol. 73, no. 6, pp. 1012–1024, Jun. 1985.

[28] L. Grant, "Diffuse and specular characteristics of leaf reflectance," *Remote Sens. Environ.*, vol. 22, pp. 309–322, 1987.

[29] L. Grant, C. S. T. Daughtry, and V. C. Vanderbilt, "Polarized and non-polarized leaf reflectances of Coleus blumei," *Environ. Exp. Botany*, vol. 24, pp. 139–145, 1987.

[30] L. Grant, C. S. T. Daughtry, and V. C. Vanderbilt, "Variations in the polarized leaf reflectance of Sorghum bicolor," *Remote Sens. Environ.*, vol. 21, pp. 333–339, 1987.

[31] A. Kallel and J. P. Gastellu-Etchegorry, "Canopy polarized BRDF simulation based on non-stationary Monte Carlo 3-D vector RT modeling," *J. Quantitative Spectrosc. Radiative Transfer*, vol. 189, pp. 149–167, 2017.

[32] B. Yang *et al.*, "Analyses of impact of needle surface properties on estimation of needle absorption spectrum: Case study with coniferous needle and shoot samples," *Remote Sens.*, vol. 8, no. 7, 2016, Art. no. 563.

[33] W. E. Martin *et al.*, "Polarized optical scattering signatures from biological materials," *J. Quantitative Spectrosc. Radiative Transfer*, vol. 111, no. 16, pp. 2444–2459, 2010.

[34] V. C. Vanderbilt and L. Grant, "Plant canopy specular reflectance model," *IEEE Trans. Geosci. Remote Sens.*, vol. GRS-23, no. 5, pp. 722–730, Sep. 1985.

[35] V. C. Vanderbilt, L. Grant, L. L. Biehl, and B. F. Robinson, "Specular, diffuse, and polarized light scattered by two wheat canopies," *Appl. Opt.*, vol. 24, no. 15, pp. 2408–2418, 1985.

[36] P. Woessner and B. Hapke, "Polarization of light scattered by clover," *Remote Sens. Environ.*, vol. 21, pp. 243–261, 1987.

[37] J. Suomalainen, T. Hakala, E. Puttonen, and J. Peltoniemi, "Polarised bidirectional reflectance factor measurements from vegetated land surfaces," *J. Quantitative Spectrosc. Radiative Transfer*, vol. 110, no. 12, pp. 1044–1056, 2009.

[38] J. I. Peltoniemi, M. Gritsevich, and E. Puttonen, "Reflectance and polarization characteristics of various vegetation types," in *Light Scattering Reviews 9: Light Scattering and Radiative Transfer*. Berlin, Germany: Springer, 2015, pp. 257–294.

[39] Z. Sun, D. Wu, Y. Lv, and Y. Zhao, "Polarized reflectance factors of vegetation covers from laboratory and field: A comparison with modeled results," *J. Geophys. Res., Atmos.*, vol. 122, no. 2, pp. 1042–1065, 2017.

[40] P. J. Curran, "The relationship between polarized visible light and vegetation amount," *Remote Sens. Environ.*, vol. 11, pp. 87–92, 1981.

[41] G. Rondeaux and M. Herman, "Polarization of light reflected by crop canopies," *Remote Sens. Environ.*, vol. 38, pp. 63–75, 1991.

[42] B. Cairns, E. E. Russell, and L. D. Travis, "The research scanning polarimeter: Calibration and ground-based measurements," *Proc. SPIE*, vol. 3754, pp. 186–197, 1999.

[43] P.-Y. Deschamps *et al.*, "The POLDER mission: Instrument characteristics and scientific objectives," *IEEE Trans. Geosci. Remote Sens.*, vol. 32, no. 3, pp. 598–615, May 1994.

[44] F. Nadal and F. M. Bréon, "Parameterization of surface polarized reflectance derived from POLDER spaceborne measurements," *IEEE Trans. Geosci. Remote Sens.*, vol. 37, no. 3, pp. 1709–1718, May 1999.

[45] P. Litvinov, O. Hasekamp, and B. Cairns, "Models for surface reflection of radiance and polarized radiance: Comparison with airborne multi-angle photopolarimetric measurements and implications for modeling top-of-atmosphere measurements," *Remote Sens. Environ.*, vol. 115, no. 2, pp. 781–792, 2011.

[46] F. M. Bréon, D. Tanré, P. Lecomte, and M. Herman, "Polarized reflectance of bare soils and vegetation: Measurements and models," *IEEE Trans. Geosci. Remote Sens.*, vol. 33, no. 2, pp. 487–499, Mar. 1995.

[47] F. Maignan, F.-M. Bréon, E. Fédèle, and M. Bouvier, "Polarized reflectances of natural surfaces: Spaceborne measurements and analytical modeling," *Remote Sens. Environ.*, vol. 113, no. 12, pp. 2642–2650, 2009.

[48] F. Waquet *et al.*, "Polarimetric remote sensing of aerosols over land," *J. Geophys. Res.*, vol. 114, no. D1, 2009, Art. no. D01206.

[49] L. Bousquet, S. Lachérade, S. Jacquemoud, and I. Moya, "Leaf BRDF measurements and model for specular and diffuse components differentiation," *Remote Sens. Environ.*, vol. 98, no. 2/3, pp. 201–211, 2005.

[50] A. Comar *et al.*, "ACT: A leaf BRDF model taking into account the azimuthal anisotropy of monocotyledonous leaf surface," *Remote Sens. Environ.*, vol. 143, pp. 112–121, 2014.

[51] D. Combes, L. Bousquet, S. Jacquemoud, H. Sinoquet, C. Varlet-Grancher, and I. Moya, "A new spectrogoniophotometer to measure leaf spectral and directional optical properties," *Remote Sens. Environ.*, vol. 109, no. 1, pp. 107–117, 2007.

[52] A. Kallel, "Leaf polarized BRDF simulation based on Monte Carlo 3-D vector RT modeling," *J. Quantitative Spectrosc. Radiative Transfer*, vol. 221, pp. 202–224, 2018.

[53] F. Baret, B. Andrieu, and G. Guyot, "A simple model for leaf optical properties in visible and near infrared: Application to the analysis of spectral shifts determinism," in *Applications of Chlorophyll Fluorescence in Photosynthesis Research, Stress Physiology, Hydrobiology and Remote Sensing*. Dordrecht, The Netherlands: Springer, 1988.

[54] W. Li, Z. Sun, S. Lu, and K. Omasa, "Estimation of the leaf chlorophyll content using multiangular spectral reflectance factor," *Plant Cell Environ.*, vol. 42, no. 11, pp. 3152–3165, Nov. 2019.

[55] J. Penuelas, F. Baret, and I. Filella, "Semi-empirical indices to assess carotenoids/chlorophyll—A ratio from leaf spectral reflectance," *Photosynthetica*, vol. 31, no. 2, pp. 221–230, 1995.

[56] B. Datt, "A new reflectance index for remote sensing of chlorophyll content in higher plants: Tests using Eucalyptus Leaves," *J. Plant Physiol.*, vol. 154, no. 1, pp. 30–36, 1999.
[57] Z. Sun, Z. Wu, and Y. Zhao, "Semi-automatic laboratory goniospectrometer system for performing multi-angular reflectance and polarization measurements for natural surfaces," *Rev. Sci. Instrum.*, vol. 85, no. 1, Jan. 2014, Art. no. 014503.
[58] G. Schaepman-Strub, M. E. Schaepman, T. H. Painter, S. Dangel, and J. V. Martonchik, "Reflectance quantities in optical remote sensing—Definitions and case studies," *Remote Sens. Environ.*, vol. 103, no. 1, pp. 27–42, 2006.
[59] S. R. Sandmeier, C. Muller, B. Hosgood, and G. Andreoli, "Sensitivity analysis and quality assessment of laboratory BRDF data," *Remote Sens. Environ.*, vol. 64, pp. 176–191, 1998.
[60] S. R. Sandmeier, C. Muller, B. Hosgood, and G. Andreoli, "Physical mechanisms in hyperspectral BRDF data of grass and watercress," *Remote Sens. Environ.*, vol. 66, pp. 222–233, 1998.
[61] J. I. Peltoniemi *et al.*, "BRDF measurement of understory vegetation in pine forests: Dwarf shrubs, lichen, and moss," *Remote Sens. Environ.*, vol. 94, no. 3, pp. 343–354, 2005.
[62] Z. Sun, Y. Huang, Y. Bao, and D. Wu, "Polarized remote sensing: A note on the Stokes parameters measurements from natural and manmade targets using a spectrometer," *IEEE Trans. Geosci. Remote Sens.*, vol. 55, no. 7, pp. 4008–4021, Jul. 2017.
[63] J. F. G. M. Wintermans and A. De Mots, "Spectrophotometric characteristics of chlorophylls a and b and their phenophytins in ethanol," *Biochimica et Biophysica Acta—Biophys. Including Photosynthesis*, vol. 109, pp. 448–453, 1965.
[64] A. A. Gitelson, Y. J. Kaufman, and M. N. Merzlyak, "Use of a green channel in remote sensing of global vegetation from EOS–MODIS," *Remote Sens. Environ.*, vol. 58, pp. 289–298, 1996.
[65] A. D. Richardson, S. P. Duigan, and G. Berlyn, "An evaluation of noninvasive methods to estimate foliar chlorophyll content," *New Phytologist*, vol. 153, pp. 185–194, 2002.
[66] H. K. Lichtenthaler, A. Gitelson, and M. Lang, "Non-destructive determination of chlorophyll content of leaves of a green and an aurea mutant of tobacco by reflectance measurements," *J. Plant Physiol.*, vol. 148, no. 3/4, pp. 483–493, 1996.
[67] B. Datt, "Remote sensing of chlorophyll a, chlorophyll b, chlorophyll a+b, and total carotenoid content in Eucalyptus leaves," *Remote Sens. Environ.*, vol. 66, pp. 111–121, 1998.
[68] G. A. Blackburn, "Quantifying chlorophylls and carotenoids at leaf and canopy scales: An evaluation of some hyperspectral approaches," *Remote Sens. Environ.*, vol. 66, pp. 273–285, 1998.
[69] Y. Zhu, D. Zhou, X. Yao, Y. Tian, and W. Cao, "Quantitative relationships of leaf nitrogen status to canopy spectral reflectance in rice," *Aust. J. Agricultural Res.*, vol. 58, no. 11, pp. 1077–1085, 2007.
[70] G. A. Blackburn, "Spectral indices for estimating photosynthetic pigment concentrations: A test using senescent tree leaves," *Int. J. Remote Sens.*, vol. 19, no. 4, pp. 657–675, 1998.
[71] Y. C. Tian, X. Yao, J. Yang, W. X. Cao, D. B. Hannaway, and Y. Zhu, "Assessing newly developed and published vegetation indices for estimating rice leaf nitrogen concentration with ground- and space-based hyperspectral reflectance," *Field Crops Res.*, vol. 120, no. 2, pp. 299–310, 2011.
[72] Z. Sun, Z. Peng, D. Wu, and Y. Lv, "Photopolarimetric properties of leaf and vegetation covers over a wide range of measurement directions," *J. Quantitative Spectrosc. Radiative Transfer*, vol. 206, pp. 273–285, 2018.
[73] F.-M. Breon and F. Maignan, "A BRDF–BPDF database for the analysis of Earth target reflectances," *Earth Syst. Sci. Data*, vol. 9, no. 1, pp. 31–45, 2017.
[74] C. L. Bradley, D. J. Diner, F. Xu, M. Kupinski, and R. A. Chipman, "Spectral invariance hypothesis study of polarized reflectance with The Ground-Based Multiangle SpectroPolarimetric Imager," *IEEE Trans. Geosci. Remote Sens.*, vol. 57, no. 10, pp. 8191–8207, Oct. 2019.
[75] A. Comar, F. Baret, F. Viénot, L. Yan, and B. de Solan, "Wheat leaf bidirectional reflectance measurements: Description and quantification of the volume, specular and hot-spot scattering features," *Remote Sens. Environ.*, vol. 121, pp. 26–35, 2012.
[76] G. G. Stokes, "On the composition and resolution of streams of polarized light from multiple sources," *Trans. Cambridge Philos. Soc.*, vol. 9, p. 399, 1852.
[77] S. Lu, X. Lu, W. Zhao, Y. Liu, Z. Wang, and K. Omasa, "Comparing vegetation indices for remote chlorophyll measurement of white poplar and Chinese elm leaves with different adaxial and abaxial surfaces," *J. Exp. Botany*, vol. 66, no. 18, pp. 5625–5637, Sep. 2015.
[78] S. Lu, F. Lu, W. You, Z. Wang, Y. Liu, and K. Omasa, "A robust vegetation index for remotely assessing chlorophyll content of dorsiventral leaves across several species in different seasons," *Plant Methods*, vol. 14, 2018, Art. no. 15.
[79] D. Li *et al.*, "Assessment of unified models for estimating leaf chlorophyll content across directional-hemispherical reflectance and bidirectional reflectance spectra," *Remote Sens. Environ.*, vol. 231, 2019, Art. no. 111240.
[80] A. Kallel, " Two-scale Monte Carlo ray tracing for canopy-leaf vector radiative transfer coupling," *J. Quantitative Spectrosc. Radiative Transfer*, vol. 243, 2020, Art. no. 106815.

Yuefeng Li received the B.S. degree from the College of Environment and Planning, Henan University, Kaifeng, China, in 2016. Since 2017, he has been working toward the Ph.D. degree with Northeast Normal University, Changchun, China.

His research interests include the polarized remote sensing, vegetation spectral index, and carbon storage in peatland.

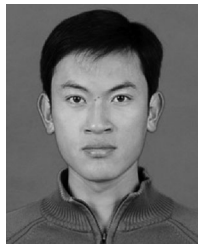

Zhongqiu Sun received the Ph.D. degree in GIS from the School of Geographical Science, Northeast Normal University, Changchun, China, in 2013.

From 2013 to 2016, he was a Research Scientist with the Laboratory of Polarized Remote Sensing, Northeast Normal University, where since 2016, he has been an Associate Professor. His research interests include the modeling of polarized remote sensing and applications of remote sensing techniques.

Shan Lu received the Ph.D. degree in bioenvironmental engineering from The University of Tokyo, Tokyo, Japan, in 2007.

From 2008 to 2016, she was an Associate Professor with the Laboratory of Polarized Remote Sensing, Northeast Normal University, Changchun, China, where since 2016, she has been a Professor. Her research interests include the modeling and analysis of polarized remote sensing, hyperspectral remote sensing and application.

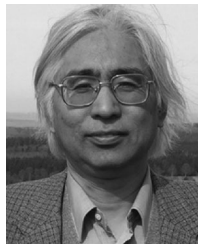

Kenji Omasa received the Ph.D. degree in engineering from The University of Tokyo, Tokyo, Japan, in 1985.

During 1999–2016, he was a Professor with the Department of Agricultural and Life Sciences, The University of Tokyo. During 2014–2017, he was an Executive Board Member of the Science Council of Japan. He is currently a Professor Emeritus with The University of Tokyo; the Dean of the Faculty of Agriculture, Takasaki University of Health and Welfare, Takasaki, Japan; the President of The Agricultural Academy of Japan; a Vice President of the Association of Japanese Agricultural Scientific Societies; and a member of the Science Council of Japan. His research interests include imaging of cell level to plants, remote sensing, modeling of ecosystems, analysis of global change effects on ecosystems, and information engineering for biological and environmental systems.

Dr. Omasa was the recipient of a Medal with Purple Ribbon awarded by Government of Japan, in 2013.